Loss or Gain of Function? Ion Channel Mutation Effects on Neuronal Firing Depend on Cell Type

Abstract (250 Words Maximum - Currently 231)

Ion channels determine neuronal excitability and disruption in ion channel properties in mutations can result in neurological disorders called channelopathies. Often many mutations are associated with a channelopathy, and determination of the effects of these mutations are generally done at the level of currents. The impact of such mutations on neuronal firing is vital for selecting personalized treatment plans for patients, however whether the effect of a given mutation on firing can simply be inferred from current level effects is unclear. The general impact of the ionic current environment in different neuronal types on the outcome of ion channel mutations is vital to understanding of the impacts of ion channel mutations and effective selection of personalized treatments. Using a diverse collection of neuronal models, the effects of changes in ion current properties on firing is assessed sytematically and for episodic ataxia type 1 associated $K_V1.1$ mutations. The effects of ion current property changes or mutations on firing is dependent on the current environment, or cell type, in which such a change occurs in. Characterization of ion channel mutations as loss or gain of function is useful at the level of the ionic current, however the effects of channelopathies on firing is dependent on cell type. To further the efficacy of personalized medicine in channelopathies, the effects of ion channel mutations must be examined in the context of the appropriate cell types.

Significant Statement (120 Words Maximum - Currently 105)

Ion channels determine neuronal excitability and mutations that alter ion channel properties result in neurological disorders called channelopathies. Although the genetic nature of such mutations as well as their effects on the ion channel's biophysical properties are routinely assessed experimentally, determination of the role in altering neuronal firing is more difficult. Computational modelling bridges this gap and demonstrates that the cell type in which a mutation occurs is an important determinant in the effects of firing. As a result, classification of ion channel mutations as loss or gain of function is useful to describe the ionic current but should not be blindly extended to firing.

Introduction (750 Words Maximum - Currently 673)

Neuronal ion channels are vital in determining neuronal excitability, action potential generation and firing patterns (Bernard and Shevell, 2008; Carbone and Mori, 2020). In particular, the properties and combinations of ion channels and their resulting currents determine the firing properties of the neuron (Pospischil et al., 2008; Rutecki, 1992). However, ion channel function can be disturb resulting in altered ionic current properties and altered neuronal firing behaviour (Carbone and Mori, 2020). Ion channel mutations are a common cause of such channelopathies and are often associated with hereditary clinical disorders (Bernard and Shevell, 2008; Carbone and Mori, 2020). The effects of these mutations are frequently determined at a biophysical level, however assessment of the impact of mutations on neuronal firing and excitability is more difficult. Experimentally, transfection of cell cultures or the generation of mutant mice lines are common approaches. Cell culture transfection does not replicate the exact interplay of endogenous currents nor does it take into account the complexity of the nervous system including factors such as expression patterns, intracellular regulation and modulation of ion channels as well as network effects. Transfected

currents are characterized in isolation and the role of these isolated currents in the context of other currents in a neuron cannot be definitively inferred. The effects of individual currents *in vivo* also depend on the neuron type they are expressed in and which roles these neurons have in specific circuits. Complex interactions between different cell types *in vivo* are neglected in transfected cell culture. Additionally, transfected currents are not present with the neuron-type specific cellular machinery present *in vivo* and are even transfected in cells of different species. Furthermore, culture conditions can shape ion channel expression (Ponce et al., 2018).

The generation of mice lines is costly and behavioural characterization of new mice lines is required to assess similarities to patient symptoms. Although the generation of mouse lines is desirable for a clinical disorder characterized by a specific ion channel mutation, this approach becomes impractical for disorders associated with a collection of distinct mutations in a single ion channel. Because of the lack of adequate experimental approaches, a great need is present for the ability to assess the impacts of ion channel mutations on neuronal firing. A more general understanding of the effects of changes in current properties on neuronal firing may help to understand the impacts of ion channel mutations. Specifically, modelling approaches can be used to assess the impacts of current property changes on firing behaviour, bridging the gap between changes in the biophysical properties induced by mutations and clinical symptoms. Conductance-based neuronal models enable insight into the effects of ion channel mutations with specific effects of the resulting ionic current as well as enabling *in silico* assessment of the relative effects of changes in biophysical properties of ionic currents on neuronal firing . The effects of altered voltage-gated potassium channel $K_V1.1$ function is of particular interest in this study as it gives rise to the $I_{K_V1.1}$ current and is associated with episodic ataxia type 1. Furthermore, modelling approaches enable predictions of the effects of specific mutation and drug induced biophysical property changes.

$K_V1.1$ channels, encoded by the *KCNA1* gene, play a role in repolarizing the action potential, neuronal firing patterns, neurotransmitter release, and saltatory conduction (D'Adamo et al., 1998) and

are expressed throughout the CNS (Tsaur et al., 1992; Veh et al., 1995; Wang et al., 1994). Altered $K_V1.1$ channel function as a result of *KCNA1* mutations in humans is associated with episodic ataxia type 1 (EA1) which is characterized by period attacks of ataxia and persistent myokymia (Parker, 1946; Van Dyke et al., 1975). Onset of EA1 is before 20 years of age (Brunt and van Weerden, 1990; Jen et al., 2007; Rajakulendran et al., 2007; Van Dyke et al., 1975) and is associated with a 10 times higher prevalence of epiletic seizures(Zuberi et al., 1999). EA1 significantly impacts patient quality of life (Graves et al., 2014). $K_V1.1$ null mice have spontaneous seizures without ataxia starting in the third postnatal week although impaired balance has been reported (Smart et al., 1998; Zhang et al., 1999) and neuronal hyperexcitability has been demonstrated in these mice (Brew et al., 2003; Smart et al., 1998). However, the lack of ataxia in $K_V1.1$ null mice raises the question if the hyperexcitability seen is representative of the effects of EA1 associated $K_V1.1$ mutations.

Using a diverse set of conductance-based neuronal models we examine the role of current environment on the impact of alterations in channels properties on firing behavior generally and for EA1 associated $K_V1.1$ mutations.

Materials and Methods

All modelling and simulation was done in parallel with custom written Python 3.8 software, run on a Cent-OS 7 server with an Intel(R) Xeon (R) E5-2630 v2 CPU.

Different Cell Models

A group of neuronal models representing the major classes of cortical and thalamic neurons including regular spiking pyramidal (RS pyramidal), regular spiking inhibitory (RS inhibitory), and fast

spiking (FS) cells were used (Pospischil et al., 2008). To each of these models, a $K_V1.1$ current ($I_{K_V1.1}$; (Ranjan et al., 2019)) was added. A cerebellar stellate cell model from (Alexander et al., 2019) is used (Cb Stellate). This model was also used with a $K_V1.1$ current ($I_{K_V1.1}$; (Ranjan et al., 2019)) in addition to the A-type potassium current (Cb stellate +$K_V1.1$) or replacing the A-type potassium current (Cb stellate $\Delta K_V1.1$). A subthalamic nucleus neuron model as described by (Otsuka et al., 2004) are used (STN) and with a $K_V1.1$ current ($I_{K_V1.1}$; (Ranjan et al., 2019)) in addition to the A-type potassium current (STN +$K_V1.1$) or replacing the A-type potassium current (STN $\Delta K_V1.1$). The properties and conductances of each model are detailed in Table 1 and the gating properties are unaltered from the original models. The properties of $I_{K_V1.1}$ were fitted to the mean wild type biophysical parameters of $K_V1.1$ (Lauxmann et al., 2021).

	RS Pyra-midal	RS Inhib-itory	FS	Cb Stellate	Cb Stellate +$K_V1.1$	Cb Stellate $\Delta K_V1.1$	STN	STN +$K_V1.1$	STN $\Delta K_V1.1$
g_{Na}	56	10	58	3.4	3.4	3.4	49	49	49
g_K	5.4	1.89	3.51	9.0556	8.15	9.0556	57	56.43	57
$g_{K_V1.1}$	0.6	0.21	0.39	-	0.90556	1.50159	-	0.57	0.5
g_A	-	-	-	15.0159	15.0159	-	5	5	-
g_M	0.075	0.0098	0.075	-	-	-	-	-	-
g_L	-	-	-	-	-	-	5	5	5
g_T	-	-	-	0.45045	0.45045	0.45045	5	5	5
$g_{Ca,K}$	-	-	-	-	-	-	1	1	1
g_{Leak}	0.0205	0.0205	0.038	0.07407	0.07407	0.07407	0.035	0.035	0.035
τ_{max_M}	608	934	502	-	-	-	-	-	-
C_m	118.44	119.99	101.71	177.83	177.83	177.83	118.44	118.44	118.44

Table 1: Cell properties and conductances of regular spiking pyramidal neuron (RS Pyramidal), regular spiking inhibitory neuron (RS Inhibitory), fast spiking neuron (FS), cerebellar stellate cell (Cb Stellate), with additional $I_{K_V1.1}$ (Cb Stellate $\Delta K_V1.1$) and with $I_{K_V1.1}$ replacement of I_A (Cb Stellate $\Delta K_V1.1$), and subthalamic nucleus neuron (STN), with additional $I_{K_V1.1}$ (STN $\Delta K_V1.1$) and with $I_{K_V1.1}$ replacement of I_A (STN $K_V1.1$) models. All conductances are given in mS/cm^2. Capacitances (C_m) and τ_{max_p} are given in pF and ms respectively.

Firing Frequency Analysis

The membrane responses to 200 equidistant two second long current steps were simulated using the forward-Euler method with a $\Delta t = 0.01$ms from steady state. Current steps ranged from 0 to 1 nA for all models except for the RS inhibitory neuron models where a range of 0 to 0.35 nA was used to ensure repetitive firing across the range of input currents. For each current step, action potentials were detected as peaks with at least 50 mV prominence and a minimum interspike interval of 1 ms. The interspike interval was computed and used to determine the instantaneous firing frequencies elicited by the current step. The steady-state firing frequency were defined as the mean firing frequency in 0.5 seconds after the first action potential in the last second of the current step respectively and was used to construct frequency-current (fI) curves.

The smallest current at which steady state firing occurs was identified and the current step interval preceding the occurrence of steady state firing was simulated at higher resolution (100 current steps) to determine the current at which steady state firing began. Firing was simulated with 100 current steps from this current upwards for 1/5 of the overall current range. Over this range a fI curve was constructed and the integral, or area under the curve (AUC), of the fI curve over this interval was computed with the composite trapezoidal rule and used as a measure of firing rate independent from rheobase.

To obtain the rheobase, the current step interval preceding the occurrence of action potentials was explored at higher resolution with 100 current steps spanning the interval. Membrane responses to these current steps were then analyzed for action potentials and the rheobase was considered the lowest current step for which an action potential was elicited.

All models exhibit tonic firing and any instances of bursting were excluded to simplify the characterization of firing.

Sensitivity Analysis and Comparison of Models

Current properties of currents common to all models (I_{Na}, I_K, I_A/$I_{K_V1.1}$, and I_{Leak}) were systematically altered in a one-factor-at-a-time sensitivity analysis for all models. The gating curves for each current were shifted ($\Delta V_{1/2}$) from -10 to 10 mV in increments of 1 mV. The slope (k) of the gating curves were altered from half to twice the initial slope. Similarly, the maximal current conductance (g) was also scaled from half to twice the initial value. For both slope and conductance alterations, alterations consisted of 21 steps spaced equally on a log_2 scale.

Model Comparison

Changes in rheobase ($\Delta rheobase$) are calculated in relation to the original model rheobase. The contrast of each AUC value (AUC_i) was computed in comparison to the AUC of the unaltered wild type model (AUC_{wt})

$$AUC_{contrast} = \frac{AUC_i - AUC_{wt}}{AUC_{wt}} \tag{1}$$

To assess whether the effects of a given alteration on $AUC_{contrast}$ or $\Delta rheobase$ are robust across models, the correlation between $AUC_{contrast}$ or $\Delta rheobase$ and the magnitude of current property alteration was computed for each alteration in each model and compared across alteration types.

The Kendall's τ coefficient, a non-parametric rank correlation, is used to describe the relationship between the magnitude of the alteration and AUC or rheobase values. A Kendall τ value of -1 or 1 is indicative of monotonically decreasing and increasing relationships respectively.

KCNA1/K_V1.1 Mutations

Known episodic ataxia type 1 associated *KCNA1* mutations and their electrophysiological characterization reviewed in (Lauxmann et al., 2021). The mutation-induced changes in $I_{K_V1.1}$ amplitude and activation slope (k) were normalized to wild type measurements and changes in activation $V_{1/2}$ were used relative to wild type measurements. The effects of a mutation were also applied to I_A

when present as both potassium currents display prominent inactivation. In all cases, the mutation effects were applied to half of the $I_{K_V 1.1}$ or I_A under the assumption that the heterozygous mutation results in 50% of channels carrying the mutation. Frequency-current curves for each mutation in each model were obtained through simulation and used to characterize firing behaviour as described above. For each model the differences in mutation AUC to wild type AUC were normalized by wild type AUC ($AUC_{contrast}$) and mutation rheobases are compared to wild type rheobase values ($\Delta rheobase$). Pairwise Kendall rank correlations (Kendall τ) are used to compare the the correlation in the effects of $K_V1.1$ mutations on AUC and rheobase between models.

Code Accessibility

The code/software described in the paper is freely available online at [URL redacted for double-blind review]. The code is available as Extended Data.

Results

Firing Characterization

The quantification of the fI curve using the AUC is seen in Figure 1A. The characterization of firing with AUC and rheobase is seen in Figure 1B, where the upper left quadrant (+ΔAUC and -Δrheobase) indicate an increase in firing, whereas the bottom right quadrant (-ΔAUC and +Δrheobase) is indicative of decreased firing. In the lower left and upper right quadrants, the effects on firing are more nuance and cannot easily be described as a gain or loss of excitability.

The diversity in the neuronal models used is seen in Figure 2. Considerable variability is seen across neuronal models both in representative spike trains and their fI curves. The models chosen all fire repetitively and do not exhibit bursting. Some models, such as Cb stellate and RS inhibitory models, display type I firing whereas others such as Cb stellate $\Delta K_V1.1$and STN models have type II firing. Other models lie on a continuum between these prototypical firing classifications.

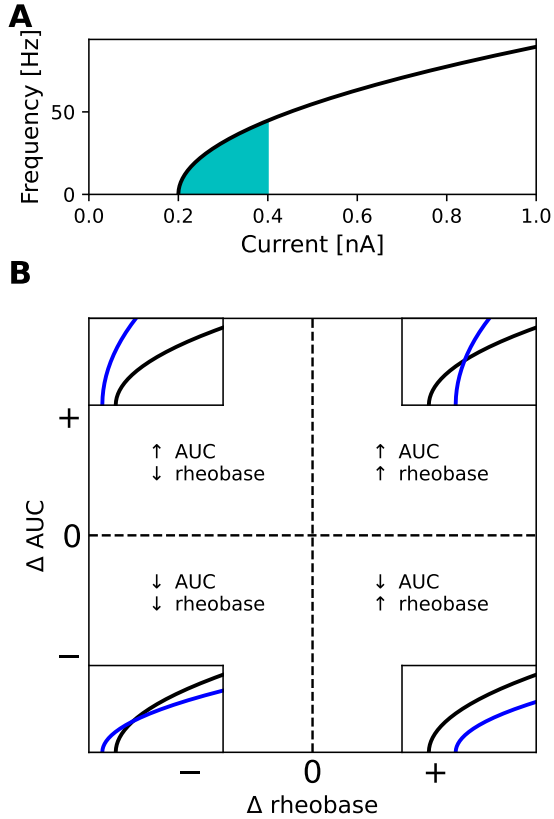

Figure 1: Characterization of firing with AUC and rheobase. (A) The area under the curve (AUC) of the repetitive firing frequency-current (fI) curve. (B) Changes in firing as characterized by ΔAUC and Δrheobase occupy 4 quadrants separated by no changes in AUC and rheobase. Representative schematic fI curves in blue with respect to a reference fI curve (black) depict the general changes associated with each quadrant.

Most neuronal models exhibit hysteresis with ascending and descending ramps eliciting spikes with different thresholds as shown by the green and red markers in Figure 2 respectively.

Sensitivity analysis

A one-factor-a-time sensitivity analysis enables the comparison of a given alteration in current parameters across models. The effect of changes in gating $V_{1/2}$ and slope factor k as well as the current conductance on AUC is shown in Figure 3 A, B and C respectively. Heterogeneity in

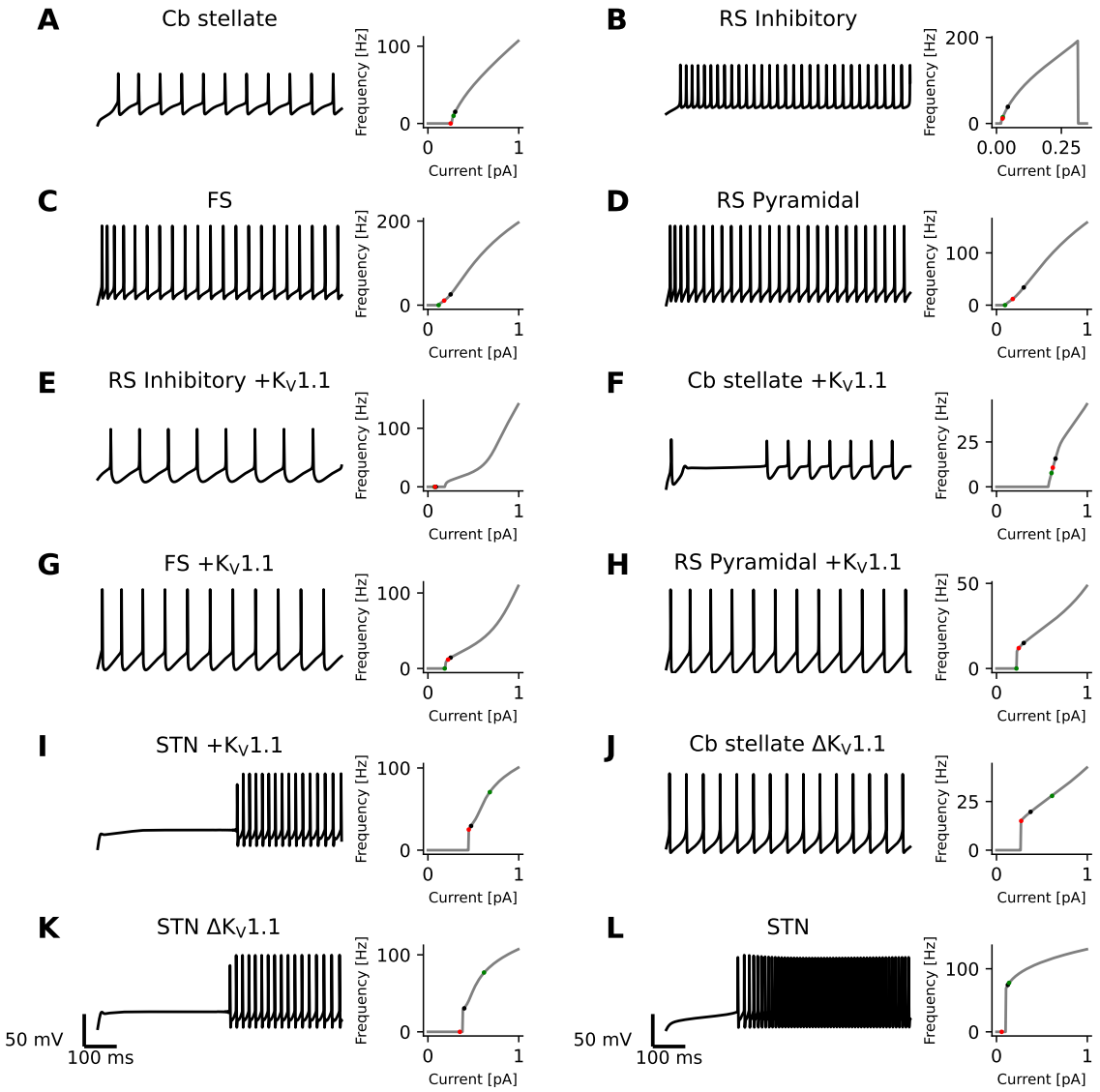

Figure 2: Diversity in Neuronal Model Firing. Spike trains (left), frequency-current (fI) curves (right) for Cb stellate (A), RS inhibitory (B), FS (C), RS pyramidal (D), RS inhibitory +K_V1.1 (E), Cb stellate +K_V1.1 (F), FS +K_V1.1 (G), RS pyramidal +K_V1.1 (H), STN +K_V1.1 (I), Cb stellate ΔK_V1.1(J), STN ΔK_V1.1(K), and STN (L) neuron models. Black marker on the fI curves indicate the current step at which the spike train occurs. The green marker indicates the current at which firing begins in response to an ascending current ramp, whereas the red marker indicates the current at which firing ceases in response to a descending current ramp (see Figure 2-1).

the correlation between gating and conductance changes and AUC occurs across models for most currents. In these cases some of the models display non-monotonic relationships (i.e. $|\text{Kendall } \tau| \neq 1$). However, shifts in A current activation $V_{1/2}$, changes in $K_V1.1$ activation $V_{1/2}$ and slope, and changes in A current conductance display consistent monotonic relationships across models.

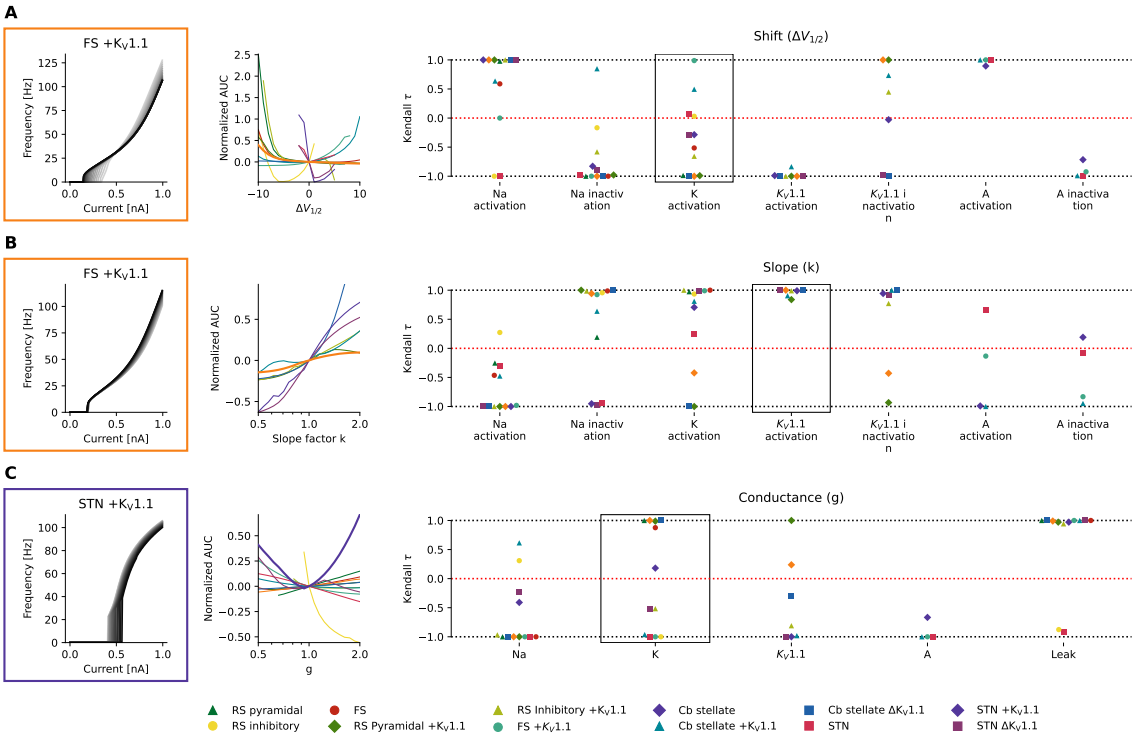

Figure 3: The Kendall rank correlation (Kendall τ) coefficients between shifts in $V_{1/2}$ and AUC, slope factor k and AUC as well as current conductances and AUC for each model are shown on the right in (A), (B) and (C) respectively. The relationships between AUC and $\Delta V_{1/2}$, slope (k) and conductance (g) for the Kendall τ coefficients highlights by the black box are depicted in the middle panel. The fI curves corresponding to one of the models are shown in the left panels.

The effect of changes in gating $V_{1/2}$ and slope factor k as well as the current conductance on rheobase is shown in Figure 4 A, B and C respectively. Shifts in half activation of gating properties are similarly correlated with rheobase across models, however Kendall τ values departing from -1

indicate non-monotonic relationships between K current $V_{1/2}$ and rheobase in some models (Figure 4A) Changes in Na current inactivation, $K_V1.1$ current inactivation and A current activation have affect rheobase with positive and negative correlations in different models (Figure 4B). Departures from monotonic relationships occur in some models as a result of K current activation, $K_V1.1$ current inactivation and A current activation in some models. Current conductance magnitude alterations affect rheobase similarly across models (Figure 4C).

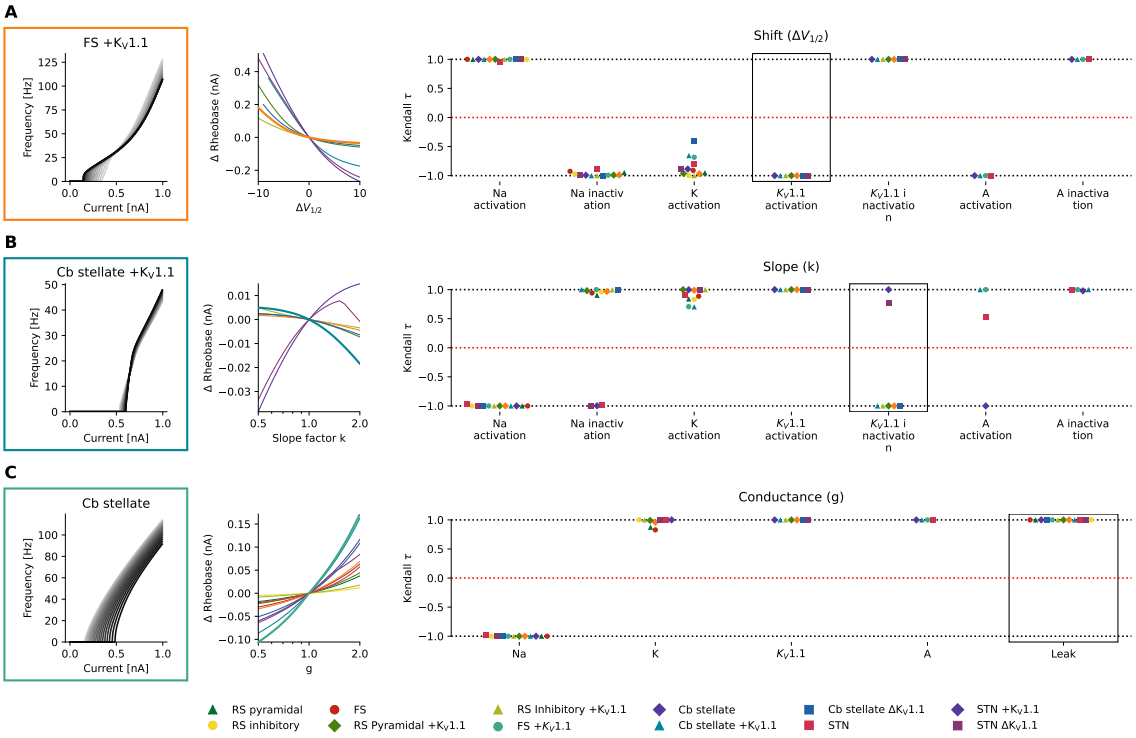

Figure 4: The Kendall rank correlation (Kendall τ) coefficients between shifts in $V_{1/2}$ and rheobase, slope factor k and AUC as well as current conductances and rheobase for each model are shown on the right in (A), (B) and (C) respectively. The relationships between rheobase and $\Delta V_{1/2}$, slope (k) and conductance (g) for the Kendall τ coefficients highlights by the black box are depicted in the middle panel. The fI curves corresponding to one of the models are shown in the left panels.

$K_V1.1$

The changes in AUC and rheobase from wild-type values for reported episodic ataxia type 1 (EA1) associated $K_V1.1$ mutations are seen in every model containing $K_V1.1$ in Figure 5A-I. Pairwise non-parametric Kendall τ rank correlations between the simulated effects of these $K_V1.1$ mutations on rheobase and AUC in different models are seen in Figure 5 J and K respectively. The effects of EA1 associated $K_V1.1$ mutations on rheobase are highly correlated across models. The effects of the $K_V1.1$ mutations on AUC are more heterogenous as reflected by both weak and strong positive and negative correlations between models Figure 5K

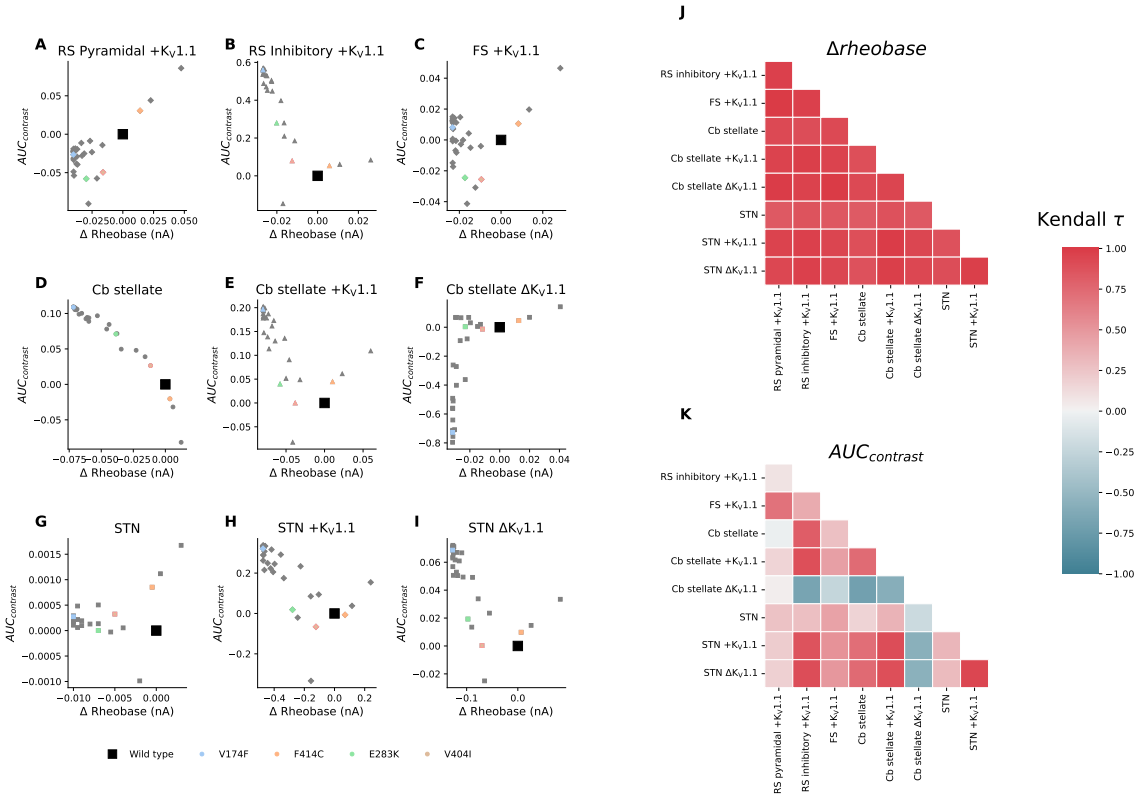

Figure 5: Effects of episodic ataxia type 1 associated $K_V1.1$ mutations on firing. Effects of $K_V1.1$ mutations on AUC ($AUC_{contrast}$) and rheobase (Δrheobase) compared to wild type for RS pyramidal +$K_V1.1$ (A), RS inhibitory +$K_V1.1$ (B), FS +$K_V1.1$ (C), Cb stellate (D), Cb stellate +$K_V1.1$ (E), Cb stellate $\Delta K_V1.1$(F), STN (G), STN +$K_V1.1$ (H) and STN $\Delta K_V1.1$(I) models V174F, F414C, E283K, and V404I mutations are highlighted in color for each model. Pairwise Kendall rank correlation coefficients (Kendall τ) between the effects of $K_V1.1$ mutations on rheobase and on AUC are shown in J and K respectively.

Discussion (3000 Words Maximum - Currently 1559)

Using a set of diverse conductance-based neuronal models, the effects of changes to current properties and conductances on firing were determined to be heterogenous for the AUC of the steady state fI curve but more homogenous for rheobase. For a known channelopathy, episodic ataxia type 1 associated $K_V1.1$ mutations, the effects on rheobase is consistent across cell types, whereas the

effect on AUC is cell type dependent.

Validity of Neuronal Models

The $K_V1.1$ model from (Ranjan et al., 2019) is based on expression of only $K_V1.1$ in CHO cells and represents the biophysical properties of $K_V1.1$ homotetramers and not heteromers. Thus the $K_V1.1$ model used here neglects the complex reality of these channels *in vivo* including their expression as heteromers and the altered biophyiscal properties of these heteromers (Coleman et al., 1999; Isacoff et al., 1990; Rettig et al., 1994; Roeper et al., 1998; Ruppersberg et al., 1990; Wang et al., 1999). Furthermore, dynamic modulation of $K_V1.1$ channels, although physiologically relevant, is neglected here. For example, $K_V\beta2$ plays a role in K_V1 channel trafficking and cell membrane expression (Campomanes et al., 2002; Manganas et al., 2001; Shi et al., 2016) and $K_V1.1$ phosphorylation increases cell membrane $K_V1.1$ (Jonas and Kaczmarek, 1996). It should be noted that the discrete classification of potassium currents into delayed rectifier and A-type is likely not biological, but rather highlights the characteristics of a spectrum of potassium channel inactivation that arises in part due to additional factors such as heteromer composition (Glasscock, 2019; Stühmer et al., 1989), non-pore forming subunits (e.g. $K_V\beta$ subunits) (Rettig et al., 1994; Xu and Li, 1997), and temperature (Ranjan et al., 2019) modulating channel properties.

Additionally, the single-compartment model does not take into consideration differential effects on neuronal compartments (i.e. axon, soma, dendrites), possible different spatial cellular distribution of channel expression across and within these neuronal compartments or across CNS regions nor does it consider different channel types (e.g $Na_V1.1$ vs $Na_V1.8$). More realistic models would consist of multiple compartments, take more currents into account and take the spatial distribution of channels into account, however these models are more computationally expensive, require current specific models and knowledge of the distribution of conductances across the cell. Despite these limitations, each of the models can reproduce physiological firing behaviour of the neurons

they represent (Alexander et al., 2019; Otsuka et al., 2004; Pospischil et al., 2008) and capture key aspects of the dynamics of these cell types.

Current Environments Determine the Effect of Ion Channel Mutations

One-factor-at-a-time (OFAT) sensitivity analyses such as the one performed here are predicated on assumptions of model linearity, and cannot account for interactions between factors (Czitrom, 1999; Saltelli and Annoni, 2010). OFAT approaches are local and not global (i.e. always in reference to a baseline point in the parameter space) and therefore cannot be generalized to the global parameter space unless linearity and additivity are met (Saltelli and Annoni, 2010). The local space around the wild type neuron is explored with an OFAT sensitivity analysis without taking interactions between parameters into account. Comparisons between the effects of changes in similar parameters across different models can be made at the wild type locale indicative of experimentally observed neuronal behaviour. In this case, the role of deviations in the ionic current properties from their wild type in multiple neuronal models presented here provides a starting point for understanding the general role of these current properties in neurons. However, a more global approach would provide a more holistic understanding of the parameter space and provide insight into interactions between properties.

Although, to our knowldege, no comprehensive evaluation of how current environment and cell type affect the outcome of ion channel mutations, comparisons between the effects of such mutations in certain cells have been reported. For instance, mutations in the SCN1A gene encoding $Na_V1.1$ result in epileptic phenotypes by selective hypoexcitability of inhibitory but not excitatory neurons in the cortex resulting in circuit hyperexcitability (Hedrich et al., 2014). Additionallly, the L858H mutation in $Na_V1.7$, associated with erythermyalgia, has been shown to cause hypoexcitability in sympathetic ganglion neurons and hyperexcitability in dorsal root ganglion neurons (Rush et al., 2006; Waxman, 2007). The differential effects of L858H $Na_V1.7$ on firing is depen-

dent on the presence or absence of another sodium channel $Na_V1.8$ (Rush et al., 2006; Waxman, 2007). In a modelling study, it was found that altering the sodium conductance in 2 stomatogastric ganglion neuron models from a population models decreases rheobase in both models, however the initial slope of the fI curves (proportional to AUC) is increased in one model and decreased in the other suggesting that the magnitude of other currents in these models (such as K_d) determines the effect of a change in sodium current (Kispersky et al., 2012). These findings, in concert with our findings suggest that the current environment in which a channelopathy occurs is vital in determining the outcomes of the channelopathy on firing.

Cell type specific differences in current properties are important in the effects of ion channel mutations, however within a cell type heterogeneity in channel expression levels exists and it is often desirable to generate a population of neuronal models and to screen them for plausibility to biological data in order to capture neuronal population diversity (Marder and Taylor, 2011). The models used here are generated by characterization of current gating properties and by fitting of maximal conductances to experimental data. This practice of fixing maximal conductances based on experimental data is limiting as it does not reproduce the variability in channel expression and neuronal firing behaviour of a heterogeneous neuron population (Verma et al., 2020). For example, a model derived from the mean conductances in a sub-population of stomatogastric ganglion ”one-spike bursting” neurons fires 3 spikes instead of 1 per burst due to an L shaped distribution of sodium and potassium conductances (Golowasch et al., 2002). Multiple sets of current conductances can give rise to the same patterns of activity also termed degeneracy and differences in neuronal dynamics may only be evident with perturbations (Goaillard and Marder, 2021; Marder and Taylor, 2011). Variability in ion channel expression often correlates with the expression of other ion channels (Goaillard and Marder, 2021) and neurons whose behaviour is similar may possess correlated variability across different ion channels resulting in stability in neuronal phenotype (Lamb and Calabrese, 2013; Soofi et al., 2012; Taylor et al., 2009). The variability of ion currents

and degeneracy of neurons may account, at least in part, for the observation that the effect of toxins within a neuronal type is frequently not constant (Khaliq and Raman, 2006; Puopolo et al., 2007; Ransdell et al., 2013).

Effects of *KCNA1* Mutations

Moderate changes in delayed rectifier potassium currents change the bifurcation structure of Hodgkin Huxley model, with changes analogous to those seen with $K_V1.1$ mutations resulting in increased excitability due to reduced thresholds for repetitive firing (Hafez and Gottschalk, 2020). Although the Hodgkin Huxley delayed rectifier lacks inactivation, the increases in excitability seen are in line with both score-based and simulation-based predictions of the outcomes of *KCNA1* mutations. Recently, (Zhao et al., 2020) predicted *in silico* that the depolarizing shifts seen as a result of *KCNA1* mutations broaden action potentials and interfere negatively with high frequency action potential firing. However, comparability of firing rates is lacking in this study. Furthermore the increased excitability seen experimentally with $K_V1.1$ null mice (Smart et al., 1998; Zhou et al., 1998), with pharmacological $K_V1.1$ block (Chi and Nicol, 2007; Morales-Villagrán et al., 1996), by (Hafez and Gottschalk, 2020) and with score-based and simulation-based predictions of *KCNA1* mutations are contrary to the claims of (Zhao et al., 2020). LOF *KCNA1* mutations generally increase neuronal excitability, however the different effects of *KCNA1* mutations across models on AUC are indicative that a certain cell type specific complexity exists.

Different current properties, such as the difference in I_A and $I_{K_V1.1}$ in the Cb stellate and STN model families alter the impact of *KCNA1* mutations on firing highlighting that knowledge of the biophysical properties of a current and its neuronal expression is vital for holistic understanding of the effects of a given ion channel mutation both at a single cell and network level.

Loss or Gain of Function Characterizations Do Not Fully Capture Ion Channel Mutation Effects on Firing

The effects of changes in current properties depend in part on the neuronal model in which they occur and can be seen in the variance of correlations (especially in AUC) across models for a given current property change. Therefore, relative conductances and gating properties of currents in the current environment in which an alteration in current properties occurs plays an important role in determining the outcome on firing. The use of loss of function (LOF) and gain of function (GOF) is useful at the level of ion channels and whether a mutation results in more or less ionic current, however the extension of this thinking onto whether mutations induce LOF or GOF at the level of neuronal firing based on the ionic current LOF/GOF is problematic due to the dependency of neuronal firing changes on the current environment. Thus the direct leap from current level LOF/GOF characterizations to effects on firing without experimental or modelling-based evidence, although tempting, should be refrained from and viewed with caution when reported. This is especially relevant in the recent development of personalized medicine for channelopathies, where a patients specific channelopathy is identified and used to tailor treatments (Ackerman et al., 2013; Gnecchi et al., 2021; Helbig and Ellis, 2020; Weber et al., 2017). However, the effects of specific ion channel mutations are often characterized in expression systems and classified as LOF or GOF to aid in treatment decisions (Brunklaus et al., 2022; Johannesen et al., 2021; Musto et al., 2020). However, this approach must be used with caution and the cell type which expressed the mutant ion channel must be taken into account. Experimental assessment of the effects of a patients specific ion channel mutation *in vivo* is not feasible at a large scale due to time and cost constraints, modelling of the effects of patient specific channelopathies is a desirable approach. Accordingly, for accurate modelling and predictions of the effects of mutations on neuronal firing, information as to the type of neurons containing the affected channel, and the properties of the affected and all currents in the affected neuronal type is needed. When modelling approaches are sought out to overcome the

limitations of experimental approaches, care must be taken to account for model dependency and the generation of relevant cell-type or cell specific populations of models should be standard in assessing the effects of mutations in specific neurons.

References

Ackerman, M. J., Marcou, C. A. and Tester, D. J. (2013), 'Personalized Medicine: Genetic Diagnosis for Inherited Cardiomyopathies/Channelopathies', *Revista Española de Cardiología (English Edition)* **66**(4), 298–307.
URL: *https://www.sciencedirect.com/science/article/pii/S1885585713000376*

Alexander, R. P. D., Mitry, J., Sareen, V., Khadra, A. and Bowie, D. (2019), 'Cerebellar Stellate Cell Excitability Is Coordinated by Shifts in the Gating Behavior of Voltage-Gated Na+ and A-Type K+ Channels', *eNeuro* **6**(3).
URL: *https://www.eneuro.org/content/6/3/ENEURO.0126-19.2019*

Bernard, G. and Shevell, M. I. (2008), 'Channelopathies: A Review', *Pediatric Neurology* **38**(2), 73–85.
URL: *https://www.sciencedirect.com/science/article/pii/S0887899407004584*

Brew, H. M., Hallows, J. L. and Tempel, B. L. (2003), 'Hyperexcitability and reduced low threshold potassium currents in auditory neurons of mice lacking the channel subunit Kv1.1', *The Journal of Physiology* **548**(1), 1–20.
URL: *https://physoc.onlinelibrary.wiley.com/doi/abs/10.1111/j..2003.t01-1-00001.x*

Brunklaus, A., Feng, T., Brünger, T., Perez-Palma, E., Heyne, H., Matthews, E., Semsarian, C., Symonds, J. D., Zuberi, S. M., Lal, D. and Schorge, S. (2022), 'Gene variant effects across sodium channelopathies predict function and guide precision therapy', *Brain* p. awac006.
URL: *https://doi.org/10.1093/brain/awac006*

Brunt, E. R. P. and van Weerden, T. W. (1990), 'Familial Paroxysmal Kinesigenic Ataxia and Continuous Myokymia', *Brain* **113**(5), 1361–1382.
URL: *https://doi.org/10.1093/brain/113.5.1361*

Campomanes, C. R., Carroll, K. I., Manganas, L. N., Hershberger, M. E., Gong, B., Antonucci, D. E., Rhodes, K. J. and Trimmer, J. S. (2002), 'Kvβ Subunit Oxidoreductase Activity and Kv1 Potassium Channel Trafficking', *Journal of Biological Chemistry* **277**(10), 8298–8305.
URL: *https://www.sciencedirect.com/science/article/pii/S0021925819364324*

Carbone, E. and Mori, Y. (2020), 'Ion channelopathies to bridge molecular lesions, channel func-

tion, and clinical therapies', *Pflügers Archiv - European Journal of Physiology* **472**(7), 733–738.
URL: *https://doi.org/10.1007/s00424-020-02424-y*

Chi, X. X. and Nicol, G. D. (2007), 'Manipulation of the Potassium Channel Kv1.1 and Its Effect on Neuronal Excitability in Rat Sensory Neurons', *Journal of Neurophysiology* **98**(5), 2683–2692.
URL: *https://journals.physiology.org/doi/full/10.1152/jn.00437.2007*

Coleman, S. K., Newcombe, J., Pryke, J. and Dolly, J. O. (1999), 'Subunit Composition of Kv1 Channels in Human CNS', *Journal of Neurochemistry* **73**(2), 849–858.
URL: *https://onlinelibrary.wiley.com/doi/abs/10.1046/j.1471-4159.1999.0730849.x*

Czitrom, V. (1999), 'One-Factor-at-a-Time versus Designed Experiments', *The American Statistician* **53**(2), 126–131.
URL: *https://www.jstor.org/stable/2685731*

D'Adamo, M. C., Liu, Z., Adelman, J. P., Maylie, J. and Pessia, M. (1998), 'Episodic ataxia type-1 mutations in the hKv1.1 cytoplasmic pore region alter the gating properties of the channel', *The EMBO Journal* **17**(5), 1200–1207.
URL: *https://www.embopress.org/doi/full/10.1093/emboj/17.5.1200*

Glasscock, E. (2019), 'Kv1.1 channel subunits in the control of neurocardiac function', *Channels* **13**(1), 299–307.
URL: *https://doi.org/10.1080/19336950.2019.1635864*

Gnecchi, M., Sala, L. and Schwartz, P. J. (2021), 'Precision Medicine and cardiac channelopathies: when dreams meet reality', *European Heart Journal* **42**(17), 1661–1675.
URL: *https://doi.org/10.1093/eurheartj/ehab007*

Goaillard, J.-M. and Marder, E. (2021), 'Ion Channel Degeneracy, Variability, and Covariation in Neuron and Circuit Resilience', *Annual Review of Neuroscience* .
URL: *https://www.annualreviews.org/doi/10.1146/annurev-neuro-092920-121538*

Golowasch, J., Goldman, M. S., Abbott, L. F. and Marder, E. (2002), 'Failure of Averaging in the Construction of a Conductance-Based Neuron Model', *Journal of Neurophysiology* **87**(2), 1129–1131.
URL: *https://journals.physiology.org/doi/full/10.1152/jn.00412.2001*

Graves, T. D., Cha, Y.-H., Hahn, A. F., Barohn, R., Salajegheh, M. K., Griggs, R. C., Bundy, B. N., Jen, J. C., Baloh, R. W., Hanna, M. G. and on behalf of the CINCH Investigators (2014), 'Episodic ataxia type 1: clinical characterization, quality of life and genotype–phenotype correlation', *Brain* **137**(4), 1009–1018.
URL: *https://doi.org/10.1093/brain/awu012*

Hafez, O. A. and Gottschalk, A. (2020), 'Altered neuronal excitability in a Hodgkin-Huxley model incorporating channelopathies of the delayed rectifier potassium channel', *Journal of Computa-*

tional Neuroscience **48**(4), 377–386.
URL: *https://doi.org/10.1007/s10827-020-00766-1*

Hedrich, U. B., Liautard, C., Kirschenbaum, D., Pofahl, M., Lavigne, J., Liu, Y., Theiss, S., Slotta, J., Escayg, A., Dihné, M., Beck, H., Mantegazza, M. and Lerche, H. (2014), 'Impaired action potential initiation in gabaergic interneurons causes hyperexcitable networks in an epileptic mouse model carrying a human nav1.1 mutation', *Journal of Neuroscience* **34**(45), 14874–14889.
URL: *https://www.jneurosci.org/content/34/45/14874*

Helbig, I. and Ellis, C. A. (2020), 'Personalized medicine in genetic epilepsies – possibilities, challenges, and new frontiers', *Neuropharmacology* **172**, 107970.
URL: *https://www.sciencedirect.com/science/article/pii/S0028390820300368*

Isacoff, E. Y., Jan, Y. N. and Jan, L. Y. (1990), 'Evidence for the formation of heteromultimeric potassium channels in Xenopus oocytes', *Nature* **345**(6275), 530–534.
URL: *https://www.nature.com/articles/345530a0*

Jen, J., Graves, T., Hess, E., Hanna, M., Griggs, R., Baloh, R. and the CINCH investigators (2007), 'Primary episodic ataxias: diagnosis, pathogenesis and treatment', *Brain* **130**(10), 2484–2493.
URL: *https://doi.org/10.1093/brain/awm126*

Johannesen, K. M., Liu, Y., Gjerulfsen, C. E., Koko, M., Sonnenberg, L., Schubert, J., Fenger, C. D., Eltokhi, A., Rannap, M., Koch, N. A., Lauxmann, S., Krüger, J., Kegele, J., Canafoglia, L., Franceschetti, S., Mayer, T., Rebstock, J., Zacher, P., Ruf, S., Alber, M., Sterbova, K., Lassuthová, P., Vlckova, M., Lemke, J. R., Krey, I., Heine, C., Wieczorek, D., Kroell-Seger, J., Lund, C., Klein, K. M., Au, P. B., Rho, J. M., Ho, A. W., Masnada, S., Veggiotti, P., Giordano, L., Accorsi, P., Hoei-Hansen, C. E., Striano, P., Zara, F., Verhelst, H., S.Verhoeven, J., Zwaag, B. v. d., Harder, A. V. E., Brilstra, E., Pendziwiat, M., Lebon, S., Vaccarezza, M., Le, N. M., Christensen, J., Schmidt-Petersen, M. U., Grønborg, S., Scherer, S. W., Howe, J., Fazeli, W., Howell, K. B., Leventer, R., Stutterd, C., Walsh, S., Gerard, M., Gerard, B., Matricardi, S., Bonardi, C. M., Sartori, S., Berger, A., Hoffman-Zacharska, D., Mastrangelo, M., Darra, F., Vøllo, A., Motazacker, M. M., Lakeman, P., Nizon, M., Betzler, C., Altuzarra, C., Caume, R., Roubertie, A., Gélisse, P., Marini, C., Guerrini, R., Bilan, F., Tibussek, D., Koch-Hogrebe, M., Perry, M. S., Ichikawa, S., Dadali, E., Sharkov, A., Mishina, I., Abramov, M., Kanivets, I., Korostelev, S., Kutsev, S., Wain, K. E., Eisenhauer, N., Wagner, M., Savatt, J. M., Müller-Schlüter, K., Bassan, H., Borovikov, A., Nassogne, M.-C., Destrée, A., Schoonjans, A.-S., Meuwissen, M., Buzatu, M., Jansen, A., Scalais, E., Srivastava, S., Tan, W.-H., Olson, H. E., Loddenkemper, T., Poduri, A., Helbig, K. L., Helbig, I., Fitzgerald, M. P., Goldberg, E. M., Roser, T., Borggraefe, I., Brünger, T., May, P., Lal, D., Lederer, D., Rubboli, G., Lesca, G., Hedrich, U. B., Benda, J., Gardella, E., Lerche, H. and Møller, R. S. (2021), 'Genotype-phenotype correlations in SCN8A-related disorders reveal prognostic and therapeutic implications', *medRxiv* p. 2021.03.22.21253711.
URL: *https://www.medrxiv.org/content/10.1101/2021.03.22.21253711v1*

Jonas, E. A. and Kaczmarek, L. K. (1996), 'Regulation of potassium channels by protein kinases',

Current Opinion in Neurobiology **6**(3), 318–323.
URL: *https://www.sciencedirect.com/science/article/pii/S0959438896801140*

Khaliq, Z. M. and Raman, I. M. (2006), 'Relative Contributions of Axonal and Somatic Na Channels to Action Potential Initiation in Cerebellar Purkinje Neurons', *Journal of Neuroscience* **26**(7), 1935–1944.

Kispersky, T. J., Caplan, J. S. and Marder, E. (2012), 'Increase in Sodium Conductance Decreases Firing Rate and Gain in Model Neurons', *Journal of Neuroscience* **32**(32), 10995–11004.
URL: *https://www.jneurosci.org/content/32/32/10995*

Lamb, D. G. and Calabrese, R. L. (2013), 'Correlated Conductance Parameters in Leech Heart Motor Neurons Contribute to Motor Pattern Formation', *PLOS ONE* **8**(11), e79267.
URL: *https://journals.plos.org/plosone/article?id=10.1371/journal.pone.0079267*

Lauxmann, S., Sonnenberg, L., Koch, N. A., Boßelmann, C. M., Winter, N., Schwarz, N., Wuttke, T. V., Hedrich, U. B. S., Liu, Y., Lerche, H., Benda, J. and Kegele, J. (2021), 'Therapeutic potential of sodium channel blockers as targeted therapy approach in KCNA1-associated episodic ataxia (EA1) and a comprehensive review of the literature', *Frontiers in Neurology* **In Press**.
URL: *https://www.frontiersin.org/articles/10.3389/fneur.2021.703970/abstract*

Manganas, L. N., Wang, Q., Scannevin, R. H., Antonucci, D. E., Rhodes, K. J. and Trimmer, J. S. (2001), 'Identification of a trafficking determinant localized to the Kv1 potassium channel pore', *Proceedings of the National Academy of Sciences* **98**(24), 14055–14059.
URL: *https://www.pnas.org/content/98/24/14055*

Marder, E. and Taylor, A. L. (2011), 'Multiple models to capture the variability in biological neurons and networks', *Nature Neuroscience* **14**(2), 133–138.
URL: *https://www.nature.com/articles/nn.2735*

Morales-Villagrán, A., Ureña-Guerrero, M. E. and Tapia, R. (1996), 'Protection by NMDA receptor antagonists against seizures induced by intracerebral administration of 4-aminopyridine', *European Journal of Pharmacology* **305**(1), 87–93.
URL: *https://www.sciencedirect.com/science/article/pii/0014299996001574*

Musto, E., Gardella, E. and Møller, R. S. (2020), 'Recent advances in treatment of epilepsy-related sodium channelopathies', *European Journal of Paediatric Neurology* **24**, 123–128.
URL: *https://www.sciencedirect.com/science/article/pii/S1090379819304295*

Otsuka, T., Abe, T., Tsukagawa, T. and Song, W.-J. (2004), 'Conductance-Based Model of the Voltage-Dependent Generation of a Plateau Potential in Subthalamic Neurons', *Journal of Neurophysiology* **92**(1), 255–264.
URL: *https://journals.physiology.org/doi/full/10.1152/jn.00508.2003*

Parker, H. L. (1946), 'Periodic ataxia', *Collected Papers of the Mayo Clinic and the Mayo Foundation. Mayo Clinic* **38**, 642–645.

Ponce, A., Castillo, A., Hinojosa, L., Martinez-Rendon, J. and Cereijido, M. (2018), 'The expression of endogenous voltage-gated potassium channels in HEK293 cells is affected by culture conditions', *Physiological Reports* **6**(8), e13663.
URL: *https://www.ncbi.nlm.nih.gov/pmc/articles/PMC5903699/*

Pospischil, M., Toledo-Rodriguez, M., Monier, C., Piwkowska, Z., Bal, T., Frégnac, Y., Markram, H. and Destexhe, A. (2008), 'Minimal Hodgkin–Huxley type models for different classes of cortical and thalamic neurons', *Biological Cybernetics* **99**(4), 427–441.
URL: *https://doi.org/10.1007/s00422-008-0263-8*

Puopolo, M., Raviola, E. and Bean, B. P. (2007), 'Roles of Subthreshold Calcium Current and Sodium Current in Spontaneous Firing of Mouse Midbrain Dopamine Neurons', *Journal of Neuroscience* **27**(3), 645–656.

Rajakulendran, S., Schorge, S., Kullmann, D. M. and Hanna, M. G. (2007), 'Episodic ataxia type 1: A neuronal potassium channelopathy', *Neurotherapeutics* **4**(2), 258–266.
URL: *https://doi.org/10.1016/j.nurt.2007.01.010*

Ranjan, R., Logette, E., Marani, M., Herzog, M., Tâche, V., Scantamburlo, E., Buchillier, V. and Markram, H. (2019), 'A Kinetic Map of the Homomeric Voltage-Gated Potassium Channel (Kv) Family', *Frontiers in Cellular Neuroscience* **13**.
URL: *https://www.frontiersin.org/articles/10.3389/fncel.2019.00358/full*

Ransdell, J. L., Nair, S. S. and Schulz, D. J. (2013), 'Neurons within the Same Network Independently Achieve Conserved Output by Differentially Balancing Variable Conductance Magnitudes', *Journal of Neuroscience* **33**(24), 9950–9956.

Rettig, J., Heinemann, S. H., Wunder, F., Lorra, C., Parcej, D. N., Oliver Dolly, J. and Pongs, O. (1994), 'Inactivation properties of voltage-gated K + channels altered by presence of β-subunit', *Nature* **369**(6478), 289–294.
URL: *https://www.nature.com/articles/369289a0*

Roeper, J., Sewing, S., Zhang, Y., Sommer, T., Wanner, S. G. and Pongs, O. (1998), 'NIP domain prevents N-type inactivation in voltage-gated potassium channels', *Nature* **391**(6665), 390–393.
URL: *https://www.nature.com/articles/34916*

Ruppersberg, J. P., Schröter, K. H., Sakmann, B., Stocker, M., Sewing, S. and Pongs, O. (1990), 'Heteromultimeric channels formed by rat brain potassium-channel proteins', *Nature* **345**(6275), 535–537.
URL: *https://www.nature.com/articles/345535a0*

Rush, A. M., Dib-Hajj, S. D., Liu, S., Cummins, T. R., Black, J. A. and Waxman, S. G. (2006), 'A single sodium channel mutation produces hyper- or hypoexcitability in different types of neurons', *Proceedings of the National Academy of Sciences* **103**(21), 8245–8250.
URL: *https://www.pnas.org/doi/10.1073/pnas.0602813103*

Rutecki, P. A. (1992), 'Neuronal excitability: voltage-dependent currents and synaptic transmission', *Journal of Clinical Neurophysiology: Official Publication of the American Electroencephalographic Society* **9**(2), 195–211.

Saltelli, A. and Annoni, P. (2010), 'How to avoid a perfunctory sensitivity analysis', *Environmental Modelling & Software* **25**(12), 1508–1517.
URL: *https://www.sciencedirect.com/science/article/pii/S1364815210001180*

Shi, X.-Y., Tomonoh, Y., Wang, W.-Z., Ishii, A., Higurashi, N., Kurahashi, H., Kaneko, S., Hirose, S. and Epilepsy Genetic Study Group, Japan (2016), 'Efficacy of antiepileptic drugs for the treatment of Dravet syndrome with different genotypes', *Brain & Development* **38**(1), 40–46.

Smart, S. L., Lopantsev, V., Zhang, C. L., Robbins, C. A., Wang, H., Chiu, S. Y., Schwartzkroin, P. A., Messing, A. and Tempel, B. L. (1998), 'Deletion of the KV1.1 Potassium Channel Causes Epilepsy in Mice', *Neuron* **20**(4), 809–819.
URL: *https://www.sciencedirect.com/science/article/pii/S0896627300810181*

Soofi, W., Archila, S. and Prinz, A. A. (2012), 'Co-variation of ionic conductances supports phase maintenance in stomatogastric neurons', *Journal of Computational Neuroscience* **33**(1), 77–95.
URL: *https://doi.org/10.1007/s10827-011-0375-3*

Stühmer, W., Ruppersberg, J., Schröter, K., Sakmann, B., Stocker, M., Giese, K., Perschke, A., Baumann, A. and Pongs, O. (1989), 'Molecular basis of functional diversity of voltage-gated potassium channels in mammalian brain.', *The EMBO Journal* **8**(11), 3235–3244.
URL: *https://www.embopress.org/doi/abs/10.1002/j.1460-2075.1989.tb08483.x*

Taylor, A. L., Goaillard, J.-M. and Marder, E. (2009), 'How Multiple Conductances Determine Electrophysiological Properties in a Multicompartment Model', *Journal of Neuroscience* **29**(17), 5573–5586.

Tsaur, M.-L., Sheng, M., Lowenstein, D. H., Jan, Y. N. and Jan, L. Y. (1992), 'Differential expression of K+ channel mRNAs in the rat brain and down-regulation in the hippocampus following seizures', *Neuron* **8**(6), 1055–1067.
URL: *https://www.sciencedirect.com/science/article/pii/089662739290127Y*

Van Dyke, D. H., Griggs, R. C., Murphy, M. J. and Goldstein, M. N. (1975), 'Hereditary myokymia and periodic ataxia', *Journal of the Neurological Sciences* **25**(1), 109–118.
URL: *https://www.sciencedirect.com/science/article/pii/0022510X75901914*

Veh, R. W., Lichtinghagen, R., Sewing, S., Wunder, F., Grumbach, I. M. and Pongs, O. (1995), 'Immunohistochemical Localization of Five Members of the KV1 Channel Subunits: Contrasting Subcellular Locations and Neuron-specific Co-localizations in Rat Brain', *European Journal of Neuroscience* **7**(11), 2189–2205.
URL: *https://onlinelibrary.wiley.com/doi/abs/10.1111/j.1460-9568.1995.tb00641.x*

Verma, P., Kienle, A., Flockerzi, D. and Ramkrishna, D. (2020), 'Computational analysis of a 9D model for a small DRG neuron', *Journal of Computational Neuroscience* **48**(4), 429–444.
URL: *https://doi.org/10.1007/s10827-020-00761-6*

Wang, F. C., Parcej, D. N. and Dolly, J. O. (1999), 'α Subunit compositions of Kv1.1-containing K+ channel subtypes fractionated from rat brain using dendrotoxins', *European Journal of Biochemistry* **263**(1), 230–237.
URL: *https://febs.onlinelibrary.wiley.com/doi/abs/10.1046/j.1432-1327.1999.00493.x*

Wang, H., Kunkel, D. D., Schwartzkroin, P. A. and Tempel, B. L. (1994), 'Localization of Kv1.1 and Kv1.2, two K channel proteins, to synaptic terminals, somata, and dendrites in the mouse brain', *Journal of Neuroscience* **14**(8), 4588–4599.
URL: *https://www.jneurosci.org/content/14/8/4588*

Waxman, S. G. (2007), 'Channel, neuronal and clinical function in sodium channelopathies: from genotype to phenotype', *Nature Neuroscience* **10**(4), 405–409.
URL: *https://www.nature.com/articles/nn1857*

Weber, Y. G., Biskup, S., Helbig, K. L., Von Spiczak, S. and Lerche, H. (2017), 'The role of genetic testing in epilepsy diagnosis and management', *Expert Review of Molecular Diagnostics* **17**(8), 739–750.
URL: *https://doi.org/10.1080/14737159.2017.1335598*

Xu, J. and Li, M. (1997), 'Kvβ2 Inhibits the Kvβ1-mediated Inactivation of K+ Channels in Transfected Mammalian Cells', *Journal of Biological Chemistry* **272**(18), 11728–11735.
URL: *https://www.sciencedirect.com/science/article/pii/S0021925818405091*

Zhang, C.-L., Messing, A. and Chiu, S. Y. (1999), 'Specific Alteration of Spontaneous GABAergic Inhibition in Cerebellar Purkinje Cells in Mice Lacking the Potassium Channel Kv1.1', *Journal of Neuroscience* **19**(8), 2852–2864.
URL: *https://www.jneurosci.org/content/19/8/2852*

Zhao, J., Petitjean, D., Haddad, G. A., Batulan, Z. and Blunck, R. (2020), 'A Common Kinetic Property of Mutations Linked to Episodic Ataxia Type 1 Studied in the Shaker Kv Channel', *International Journal of Molecular Sciences* **21**(20), 7602.
URL: *https://www.mdpi.com/1422-0067/21/20/7602*

Zhou, L., Zhang, C.-L., Messing, A. and Chiu, S. Y. (1998), 'Temperature-Sensitive Neuromuscular Transmission in Kv1.1 Null Mice: Role of Potassium Channels under the Myelin Sheath in Young Nerves', *Journal of Neuroscience* **18**(18), 7200–7215.
URL: *https://www.jneurosci.org/content/18/18/7200*

Zuberi, S. M., Eunson, L. H., Spauschus, A., De Silva, R., Tolmie, J., Wood, N. W., McWilliam, R. C., Stephenson, J. P. B., Kullmann, D. M. and Hanna, M. G. (1999), 'A novel mutation in the human voltage-gated potassium channel gene (Kv1.1) associates with episodic ataxia type 1 and

sometimes with partial epilepsy', *Brain* **122**(5), 817–825.
URL: *https://doi.org/10.1093/brain/122.5.817*

Figure/Table/Extended Data Legends

Figure 1: Characterization of firing with AUC and rheobase. (A) The area under the curve (AUC) of the repetitive firing frequency-current (fI) curve. (B) Changes in firing as characterized by ΔAUC and Δrheobase occupy 4 quadrants separated by no changes in AUC and rheobase. Representative schematic fI curves in blue with respect to a reference fI curve (black) depict the general changes associated with each quadrant.

Figure 2: Diversity in Neuronal Model Firing. Spike trains (left), frequency-current (fI) curves (right) for Cb stellate (A), RS inhibitory (B), FS (C), RS pyramidal (D), RS inhibitory +K_V1.1 (E), Cb stellate +K_V1.1 (F), FS +K_V1.1 (G), RS pyramidal +K_V1.1 (H), STN +K_V1.1 (I), Cb stellate ΔK_V1.1(J), STN ΔK_V1.1(K), and STN (L) neuron models. Black marker on the fI curves indicate the current step at which the spike train occurs. The green marker indicates the current at which firing begins in response to an ascending current ramp, whereas the red marker indicates the current at which firing ceases in response to a descending current ramp.

Figure 3: The Kendall rank correlation (Kendall τ) coefficients between shifts in $V_{1/2}$ and AUC, slope factor k and AUC as well as current conductances and AUC for each model are shown on the right in (A), (B) and (C) respectively. The relationships between AUC and $\Delta V_{1/2}$, slope (k) and conductance (g) for the Kendall τ coefficients highlights by the black box are depicted in the middle panel. The fI curves corresponding to one of the models are shown in the left panels.

Figure 4: The Kendall rank correlation (Kendall τ) coefficients between shifts in $V_{1/2}$ and rheobase, slope factor k and AUC as well as current conductances and rheobase for each model are shown on the right in (A), (B) and (C) respectively. The relationships between rheobase and $\Delta V_{1/2}$, slope (k) and conductance (g) for the Kendall τ coefficients highlights by the black box are depicted in the middle panel. The fI curves corresponding to one of the models are shown in the left panels.

Figure 5: Effects of episodic ataxia type 1 associated K_V1.1 mutations on firing. Effects of K_V1.1 mutations on AUC ($AUC_{contrast}$) and rheobase (Δrheobase) compared to wild type for RS pyramidal +K_V1.1 (A), RS inhibitory +K_V1.1 (B), FS +K_V1.1 (C), Cb stellate (D), Cb stellate +K_V1.1 (E), Cb stellate ΔK_V1.1(F), STN (G), STN +K_V1.1 (H) and STN ΔK_V1.1(I) models V174F, F414C, E283K, and V404I mutations are highlighted in color for each model. Pairwise Kendall rank correlation coefficients (Kendall τ) between the effects of K_V1.1 mutations on rheobase and on AUC are shown in J and K respectively.

Tables

	RS Pyra-midal	RS Inhib-itory	FS	Cb Stellate	Cb Stellate +K_V1.1	Cb Stellate ΔK_V1.1	STN	STN +K_V1.1	STN ΔK_V1.1
g_{Na}	56	10	58	3.4	3.4	3.4	49	49	49
g_K	5.4	1.89	3.51	9.0556	8.15	9.0556	57	56.43	57
$g_{K_V 1.1}$	0.6	0.21	0.39	-	0.90556	1.50159	-	0.57	0.5
g_A	-	-	-	15.0159	15.0159	-	5	5	-
g_M	0.075	0.0098	0.075	-	-	-	-	-	-
g_L	-	-	-	-	-	-	5	5	5
g_T	-	-	-	0.45045	0.45045	0.45045	5	5	5
$g_{Ca,K}$	-	-	-	-	-	-	1	1	1
g_{Leak}	0.0205	0.0205	0.038	0.07407	0.07407	0.07407	0.035	0.035	0.035
τ_{max_M}	608	934	502	-	-	-	-	-	-
C_m	118.44	119.99	101.71	177.83	177.83	177.83	118.44	118.44	118.44

Table 1: Cell properties and conductances of regular spiking pyramidal neuron (RS Pyramidal), regular spiking inhibitory neuron (RS Inhibitory), fast spiking neuron (FS), cerebellar stellate cell (Cb Stellate), with additional $I_{K_V 1.1}$ (Cb Stellate ΔK_V1.1) and with $I_{K_V 1.1}$ replacement of I_A (Cb Stellate ΔK_V1.1), and subthalamic nucleus neuron (STN), with additional $I_{K_V 1.1}$ (STN ΔK_V1.1) and with $I_{K_V 1.1}$ replacement of I_A (STN K_V1.1) models. All conductances are given in mS/cm^2. Capacitances (C_m) and τ_{max_p} are given in pF and ms respectively.

Extended Data

Extended Data 1: TODO: Caption for code in zip file.

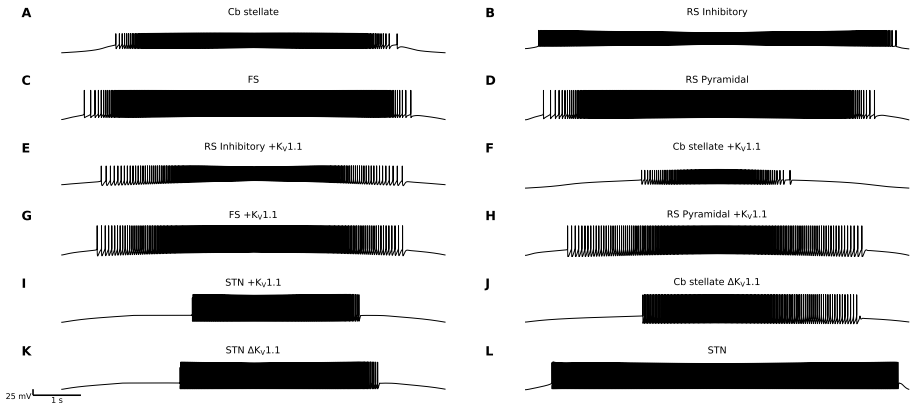

Figure 2-1: Diversity in Neuronal Model Firing Responses to a Current Ramp. Spike trains for Cb stellate (A), RS inhibitory (B), FS (C), RS pyramidal (D), RS inhibitory +K_V1.1 (E), Cb stellate +K_V1.1 (F), FS +K_V1.1 (G), RS pyramidal +K_V1.1 (H), STN +K_V1.1 (I), Cb stellate ΔK_V1.1(J), STN ΔK_V1.1(K), and STN (L) neuron models in response to a slow ascending current ramp followed by the descending version of the current ramp. The current at which firing begins in response to an ascending current ramp and the current at which firing ceases in response to a descending current ramp are depicted on the frequency current (fI) curves in Figure 2 for each model.